Dense energy carrier assessment of four combustible metal powders

Sustainable Energy Technologies and Assessments 30 (2018) 52–58

Contents lists available at ScienceDirect

Sustainable Energy Technologies and Assessments

journal homepage: www.elsevier.com/locate/seta

Dense energy carrier assessment of four combustible metal powders

Luc Dirven[a], Niels G. Deen[a], Michael Golombok[a,b,*]

[a] Eindhoven University of Technology, PO Box 513, 5600 MB Eindhoven, The Netherlands
[b] Shell Global Solutions International B.V., Grasweg 31, 1031 HW Amsterdam, The Netherlands

ARTICLE INFO

Keywords:
Energy carrier
Metal powder
Cycle efficiency
Dry route

ABSTRACT

Metal powders show great potential as dense energy carriers. This conceptual cycle for application presents a number of challenges which we address in this paper. In this study we narrowed down on four readily available promising candidates: aluminium, silicon, iron and zinc. Based on static power generation we estimated amounts required, transportation, cycle efficiency and physical explosion hazards. The scale required for transportation is much larger than in the current metal powder industry. The shipping requirements are comparable to coal. The handling hazards are only serious for aluminium. Iron and silicon emerge as the materials of choice.

Introduction

Current energy scenarios envision a society less dependent on fossil fuels and making much more use of renewable energy. This requires that we address the intermittency of renewable sources as well as the geographical mismatch between supply and demand of renewable power. An example is high-intensity solar power. In densely populated areas such as China, India and Europe the solar irradiation is substantially less than in areas such as Australia and Africa. To transport the energy to areas where it is needed, a commodity to store and globally trade energy is required: a dense energy carrier (DEC).

A DEC has two essential properties: a high energy density, and it is convenient to transport. For sustainability, the storage cycle should be regenerative, and no greenhouse gases should be emitted. Examples of energy carriers include:

- Batteries: a regenerative energy carrier, but with a limited lifetime. Batteries have a low energy density which make them prohibitive to use for large-scale storage and global transportation of energy.
- Hydrogen: an energy carrier which can be generated from water electrolysis. The current cycle efficiency is relatively low. Additionally hydrogen has to be compressed and cooled in storage which requires energy.

A recent proposal by Bergthorson [1] considers metal powder as a dense energy carrier (DEC). In a metal DEC cycle, energy is stored in such a metal powder. The complete cycle is shown in Fig. 1. At the power generation plant, metal powder is burned to generate heat which is converted to electricity. The combustion of the metal generates metal-oxide powder that is captured and transported to the regeneration plant. At the regeneration plant, the metal-oxide powder is reduced by using renewable energy. In this process, energy is stored in the metal powder, and the powder can be transported to the power generation plant where it is burned in the next cycle to produce electricity. The metal powder cycle also can be defined as an energy storage medium i.e. it captures energy that can be produced for later use. However the high density of the storage and its relative ease in transportability – as we shall see below – raise it to the status of candidate dense energy carrier.

The economics of this process rely on the mismatch between the locations of for example high intensity solar irradiation for regeneration, and world areas with high population density and industrial growth. An initial investment is required for the metal which becomes “fixed capital” – and for the purposes of this study is assumed not to deplete. The amount of powder in storage then depends on variables, such as the power supply of the regeneration plant (assumed to be “for free”), the electricity demand at the consumer side, the load size of the transportation vessel and the lead time of transportation. We assume transport between lands not too far apart. For example if we consider power demand, this peaks in winter in the Netherlands whereas solar PV power peaks in Morocco in the summer. The economic incentive is the levelling of the intermittent supply and demand of power by storage in metal powder.

One of the challenges identified in enabling the metal DEC cycle is thus transport and handling of the powders. These processes are potentially hazardous, and the scales that would be involved are significantly greater than currently applicable in the metal powder industry. The aim of this study is to address these concerns. Section

* Corresponding author at: Eindhoven University of Technology, PO Box 513, 5600 MB Eindhoven, The Netherlands.
E-mail address: michael.golombok@shell.com (M. Golombok).

https://doi.org/10.1016/j.seta.2018.09.003
Received 12 April 2018; Received in revised form 9 August 2018; Accepted 5 September 2018

Nomenclature

Symbols

E	energy content
ΔH	enthalpy difference of a process
K_{st}	deflagration index
m	mass
P	power
p	pressure
T	temperature
t	time
t_l	lead time
P	power
V	volume

greek

H	efficiency

sub/superscripts

c	cold
com	combustion
ld	load
HFO	heavy fuel oil
h	hot
M	metal
MO	metal-oxide
od	heat transfer
pg	power generation
rg	regeneration
r	reduction
tr	transportation
tot	total

abbreviations

BOE	barrel of oil equivalent
CLC	chemical looping combustion
DEC	dense energy carrier
FC	fuel consumption
HC	hydrocarbon
HV	higher heating value
MEP	maximum explosion pressure
MRP	maximum rate of pressure rise

"Background" briefly reviews the background to metal powder combustion. Section "Materials" considers material constraints. Section "Application analysis" reviews the three main issues: after a demonstration example in large scale power generation with the implications, we estimate the cycle efficiency and evaluate the main hazard which is explosion.

Background

The idea of using solid powdered fuels has existed for over a century – the nearest analogues are of course coal fired power stations. Rudolf Diesel experimented with coal dust in a diesel engine [2]. He already faced the inherent issues of solid fuels: his engine plugged up by dust build-up and the internal components suffered from severe erosion. Nonetheless, almost a century later, the vice chairman of General Motors still claimed [3] that commercial coal-powered vehicles would be "products of the next century".

Although an internal combustion engine fuelled by powder was never realised, powders are used for a variety of other applications. For example, metal powders are applied in nanofluids, gelled propellants, solid propellants, solid fuels and thermites [4]. The potential of metal powder as an energy carrier has recently gained more interest [5,6]. There have been two main routes identified: Metal powder combustion ("dry route") which produces metal oxides [7] and the "wet route" reaction with water which yields hydrogen [8]. For the latter process aluminium and magnesium are the best performers although the rate is limited by the formation of protective (effectively "anodized") oxide layers [9,10]. A major factor is the way the metal needs to be prepared for the process to enable reasonable reaction rates [11]. This corresponds to an increase in the energy cost of the regenerative step of the cycle (see below). In this study we are only concerned with the dry route as we seek a replacement combustion reaction in for example coal fired power stations, rather than assuming a whole new infrastructure that would be associated with hydrogen replacing natural gas. A large part of our study does concern the reduction aspects and so is relevant to the wet as well as the dry cycle on which we now concentrate.

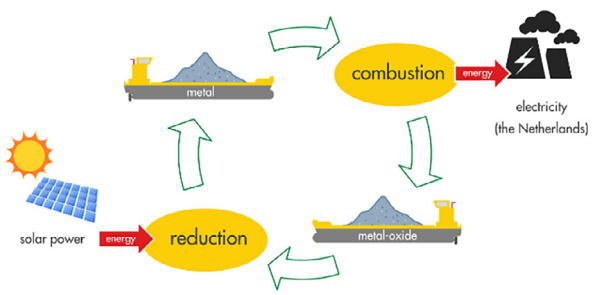

Fig. 1. The outline of the regenerative process of energy storage in metal powder. Renewables power reduction of metal oxides which are then shipped to power stations.

The combustion of metal is similar to the metal-air reaction in chemical looping combustion (CLC). CLC can be used in carbon capture and storage (CCS) systems [12]. The purpose of CLC is to obtain a pure stream of CO_2 from the combustion of (hydro)carbons. A typical CLC system is based on two reaction mechanisms. The first reaction involves the oxidation of a metal (M) with air, shown in Eq. (1a). This reaction results in a gas stream of pure nitrogen and solid metal-oxide particles.

$$xM + \frac{y}{2}O_2 \rightarrow M_xO_y + Q_1 \tag{1a}$$

where Q_1 is the exothermicity of the direct metal oxidation. The second reaction (in chemical looping combustion) involves the oxidation of a (hydro)carbon with the metal-oxide particles

$$C_iH_j + \frac{4i+j}{2y}M_xO_y \rightarrow iCO_2 + \frac{j}{2}H_2O + \frac{x(4i+j)}{2y}M(s) + Q_2 \tag{1b}$$

In this second reaction, the metal-oxide particles are reduced, and the fuel is oxidized. Of course if one balances the first and second reactions for one mole of hydrocarbon then the sum of the energies corresponds to the heating value (HV) of the hydrocarbon. In general $Q_1 \gg HV$ so the combustion of metals is certainly interesting from an energetic point of view [10]. The two reactions for chemical looping combustion take place in separate reactors and nitrogen and CO_2 are obtained separately. CLC shows similarities with the metal DEC cycle, but there are also some fundamental differences. Firstly, the main goal of CLC and the metal DEC cycle differs. In CLC, the main goal is to obtain a separate CO_2 stream for CCS. The main goal of the metal DEC cycle is to transport and store energy. Secondly, in CLC the oxidation

and reduction take place in separate reactors, but within a single plant. In the metal DEC cycle, the oxidation and reduction take place at separate locations. Finally, the oxidation and reduction in CLC occur on the surface of the particles [12]. The particle is not fully oxidized or reduced. If we want to use metal powder as an energy carrier, the particle should definitely be reduced and oxidized as near completely as practicable. If not, efficiency losses occur. There is also a rather complex behaviour of metal particles on burning [7,13]. For example nanoparticles can be produced which are bad for emissions and material loss [14]. Moreover, there is more of a problem with passivating oxide layers when one is dealing with smaller particles [10]. These can constitute more than a third of the nanoparticles, however the main concern here is their high spontaneous ignition risk which we discuss below.

Experiments with metal powder as a fuel have been done for other applications e.g. aluminium powder as a fuel for a ramjet [15]. An optimal combustion efficiency of 73% was found. In this experiment, spherical aluminium particles with an average diameter of 20 μm were used. In general, combustion efficiencies in a flame for micron-sized metal particles are poor. However this restriction only applies to the ramjet application where the high flow leads to a restricted residence time in the flame. Combustion in a boiler system at longer residence times should achieve 100% combustion efficiency for the purposes of the envisaged application. The addition of nanoparticles to the fuel mixture can improve combustion efficiency [4] but yields problems for combustion product removal (see below).

Materials

A good metal dense energy carrier (DEC) by definition has a high specific energetic content and low mass density. It should be abundant in the earth's crust. Comparison of % mass abundances show that silicon (28 wt%), aluminium (8 wt%), and iron (5 wt%) are the most common materials in the lithosphere [5]. Bergthorson found that iron has beneficial combustion properties [1]. Strictly speaking, silicon is not a metal, but for the purposes of this study is referred to as such. Zinc (0.007 wt%) is added to the list of materials despite the fact that it is not abundant. The inclusion of Zn is justified on the materiality criterion of Kramer and Haigh [16]. Based on a meta-data analysis, they postulate a first law that new technologies impinge on the market negligibly as they exponentially grow until they deliver 1% of the energy. At this point the technology reaches “materiality”. On a local level in the Netherlands, the zinc producer Nyrstar uses about 1% of all Dutch energy for electrolysis. A technology which delivers the energy to do this will have achieved local materiality – so zinc is added to the list for this study.

An additional requirement is that the metal should be strongly reactive with oxygen at high temperatures and not at low temperatures. A previous study has ranked all these metals in terms of reactivity with water for the purposes of the “wet cycle” discussed above [17]. The hydrogen yield per unit mass, the activation energy and (thus also the temperature sensitivity) were ranked Al > Si > Zn > Fe whereas for volumetric sensitivity and conversion completeness, Zn and Si change order in that list. (In fact in general the values of all parameters are close to one another for Zn and Si.)

The weight and volume of a unit of energy are derived from the heating value of the material. In Fig. 2 the weight and volume of one barrel of oil equivalent (BOE) of energy are shown for the metals and compared to oil, coal, gasoline and liquefied natural gas (LNG). The higher heating value is used for the (hydro)carbons (HC). (Metals do not have a distinct lower and higher heating value since no condensable products are formed in metal-air combustion.) The heating value of the metals is calculated using the simplified reaction mechanisms of combustion and the enthalpy of formation of the resulting oxide. From Fig. 2 it can be seen that a barrel of oil (energy) equivalent (BOE) for Al, Si and Fe have lower volumes than (hydro)carbons – this is a reflection of the higher densities of the metals and their higher heating values. The ordering for mass densities is HC ≪ Si < Al ≪ Zn < Fe. This explains why the masses of Zn and Fe are much higher for one BOE.

The BOE plot from Fig. 2 does not give a fair comparison with hydrocarbons for this type of application since the mass of the metal-oxides is greater than the mass of the metals. Additionally, the specific density of the solid material is used in Fig. 2. Powders have a lower bulk density than the solid density [18]. The decrease in density depends on the shape of the particles, which is unknown. In this case, it is assumed that the particles are spherical. The limit for compact random packing of spherical particles is $\varphi = 0.74$ [19]. The bulk volume of the metal powder containing one BOE of energy increases if (for metal variation) the metal molecular mass increases or the packing of the particles decreases – the latter case corresponding to a reduction in bulk mass density leading to a larger bulk volume for the same mass. This is now discussed in our large power station example analysis.

Application analysis

Static power

An example case is analysed to benchmark the performance of metal powders as a DEC. The metal powder is used to fuel a 1 GW_{th} power plant. Coal is used to benchmark the performance of the metals because it is a conventional energy source for large-scale power plants. In analogy to coal, the metal powder is transported by ship. A bulk carrier with a capacity of 100,000 tonnes is considered. The number of bulk carriers required annually for each material is shown in Fig. 3. The solid bars indicate the number of bulk carriers required to transport the metal. The hatched bars indicate the bulk carriers required to transport the metal-oxide in the opposite direction. More bulk carriers are required for the metal-oxide powder transportation than for the metal powder because the total mass of the metal-oxide powder is higher. For coal combustion CO_2 is not shipped because in conventional combustion CO_2 is emitted into the atmosphere. A fair comparison would require that the energy required for CO_2 capture and storage (CCS) should be estimated.

The number of bulk carriers required for Zn and Fe is significantly higher than for coal, Al and Si. This reduces the total cycle efficiency because more energy is needed for transport.

Cycle efficiency

The efficiency of the metal dense energy carrier cycle depends on three main processes: the combustion at the power generation plant η_{pg} (this includes the combustion efficiency and the heat transfer – see below), the reduction of the metal-oxides at the regeneration plant η_{rg} and the transportation of the powders η_{tr}. The total cycle efficiency is:

$$\eta_{tot} = \eta_{pg} \cdot \eta_{rg} \cdot \eta_{tr} \quad (2)$$

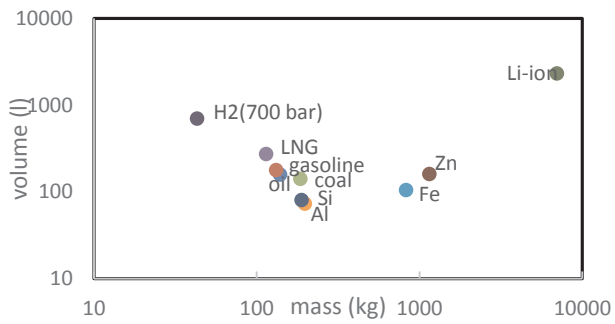

Fig. 2. The weight and volume of one barrel of oil equivalent of energy for a range of metals and hydrocarbon products.

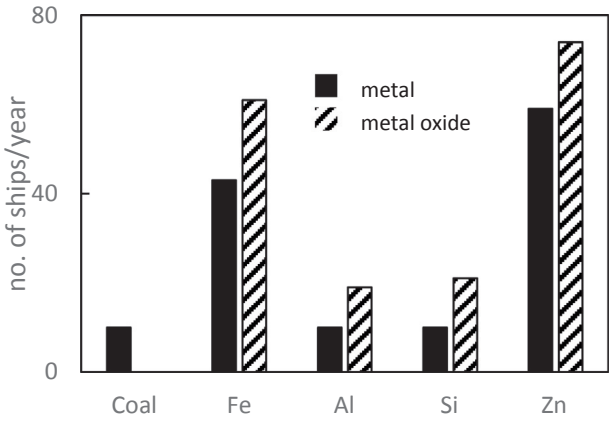

Fig. 3. The number of 100,000 tonne ships per year required to fuel a 1 GW_{th} power plant.

Power generation

We here analyse the term η_{pg} which is further broken down into components. If the metal powder is completely burned, the energy released is the heating value equated to the heat of combustion ΔH_c. The thermal energy in the hot flue gases is transferred to electrical energy in a power cycle. However, not all the heat released by combustion for work generation η_{com} is transferred to the gas as some of the heat is retained in the metal-oxide particles. The heat transfer efficiency η_{od} is defined as the fraction of heat transferred to the flue gases:

$$\eta_{od} = 1 - \frac{m_{MO} c_{p,MO} \Delta T}{\Delta H_c} \tag{3}$$

where m_{MO} is the mass of metal-oxide produced per kg of metal, $c_{p,MO}$ is the heat capacity of the metal-oxide and ΔT is the temperature increase due to combustion. It is assumed that this has a constant value for comparison $\Delta T = 1200$ K and we have also assumed constant values for the heat capacity c_p. We also assume that the hypothetical power cycle is able to extract the heat from the oxide particles. The hot particles can be removed for example by cyclones. The heat retained in the metal-oxide particles after separation can be recovered for the working fluid of the power cycle.

Of course it is all very well transferring heat to the flue gases, there still remains the classical problem of efficiently transferring the heat to the working fluid. We can consider a conventional cycle efficiency $\eta_{com} = 40\%$ consisting of the theoretical Carnot efficiency multiplied by the efficiency of various heat recovery processes typically included in for example, reheat and combined cycles as well as exhaust heat recovery.

In terms of the Carnot efficiency, it is perhaps worth noting that the steel material properties limit the maximum temperature that can be allowed. Metal combustion has considerably higher adiabatic temperatures than hydrocarbons [1]. If a power cycle could be developed that could operate at these temperatures e.g. with ceramic materials, a significant increase in power cycle efficiency could be gained. Metals thus have the potential, with correct material choices such as ceramics, to yield considerably higher efficiencies [1]. For now we use the standard value to generate the total power generation efficiency given by

$$\eta_{pg} = \eta_{od}\, \eta_{com} \tag{4}$$

Regeneration

The regeneration of metals from metal oxides corresponds to the smelting process in current industrial practice. The efficiency here can encompass a number of subsidiary factors including the energy input to generate a quantity of metal. This might include overcoming restrictions that require operation at higher temperatures or reduced pressures [20]. Since we are assuming an unrestricted amount of surplus renewable energy for the metals reduction, the consideration of efficiency reduces to a purely electrochemical one where we can define the efficiency as the heating value of the metal generated as a fraction of the energy required for the electrochemical process.

Palumbo et al. [20] developed such a scheme for a hydrogen generation process powered by electrochemical partial reduction of metal oxides. They derive a maximum thermal efficiency for the case when the only energy not recovered is that used to drive the reduction reaction. In our case this becomes the heating value of the recovered metal HV_m divided by the theoretical electrical energy (ΔG_{red}) used for recovery.

$$\eta_{rg} = \frac{HV_m}{\Delta G_{red}} \tag{5}$$

where the denominator can be derived from the electrochemical potentials of the reaction. These compare with the raw energies for the smelting process [6,21–23].

Transportation

As is standard for hydrocarbon (including LNG) transport efficiency, we identify the fuel burnt as the operational transportation losses. In the case of hydrocarbons (and by definition where some carried fuel is used for propulsion such in LNG tankers) the amount of fuel left over after the journey as a fraction of that loaded at the beginning gives the transport efficiency. Complementarily, the efficiency loss in transport η_l is the ratio of the energy required for the shipping divided by the energetic content of the load (E_{ld}). If the power consumption of the ship (expressed here as fuel consumption) is P_{tr}, then the energy of fuel burnt during a journey of duration t_L is given by $t_L\, P_{tr}$. The efficiency loss is then given by

$$\eta_l = t_L \cdot \frac{P_{tr}}{E_{ld}} \tag{6}$$

The power is estimated by evaluating the fuel consumption (FC) of the ship. The fuel considered is heavy fuel oil (HFO) with known marine carrier fuel consumption. The heating value of the fuel HV_{HFO} and the total fuel consumption FC_{tot} determine the energy required for shipping. The total fuel consumption is the sum of the fuel consumption for the metal powder shipping and the metal-oxide powder shipping. A heating value of 20 MJ kg^{-1} was assumed for the HFO. The power required for shipping transportation is:

$$P_{tr} = [FC_M + FC_{MO}] \cdot HV_{HFO} \tag{7}$$

The energetic content of the load is calculated from the heating value of the metal, HV_M, and the load size of the ship, m_{ld}. The load size of the bulk carrier is 100,000 tonnes. The energetic content of the load is:

$$E_{ld} = m_{ld} HV_m \tag{8}$$

The transport efficiency is found by substituting Eqs. (7) and (8) in Eq. (6):

$$\eta_{tr} = 1 - \eta_l = 1 - t_l \frac{(FC_M + FC_{MO}) HV_{HFO}}{m_{ld} HV_M} \tag{9}$$

The lead time of transportation obviously is confined to a lead time to keep the operation profitable i.e. $0 \le \eta_l \ll 1$ since the definition is in terms of fraction of load energy consumed during the journey. The fuel consumption depends on a variety of factors: An estimate is done by evaluating the average fuel consumption of a similar size container vessel cruising 700–1000 km per day [24]. The fuel consumption is estimated to be FC = 100 tonnes per day.

Fig. 4 shows the second term on the right hand side of Eq. (9) i.e. the fraction of loaded energy lost in carrier transport as a function of lead time. The range of transportation efficiencies varies between 92% and 99%. The efficiency loss for Al and Si is substantially less than for Fe

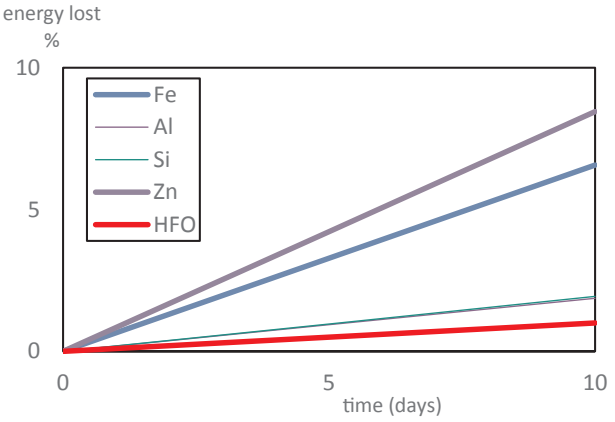

Fig. 4. Fraction of transported energy carrier content lost. Note That Si and Al nearly superimpose one another.

and Zn due to the higher energetic content of the load. Oil is even more efficient than Al and Si because no material is recycled i.e. no CO_2 capture, return and fixture. Oil is only shipped to where it is needed and the combustion products are emitted into the atmosphere. If the CO_2 was shipped back to the well, the efficiency would decrease significantly.

The cycle efficiency should be interpreted as a rough estimate. The reduction efficiency was derived from similar metal smelting processes and only Zn and Al are industrially reduced using electrolysis. Silicon and iron are reduced using coal. The energy use of these smelting plants also includes many other processes than reduction such as filtering and cleaning of the ore. If the cycle (Fig. 1) is closed and all material is recycled, then reduction can be more efficient.

Cycle efficiency

Combining the efficiencies of each of the three steps – power generation, recycling and transportation – each of the components and the total results are shown in Fig. 5.

The heat transfer differences decrease somewhat with the increasing molecular weight – larger masses absorb more heat. The transportation losses have already been discussed and are relatively small. It is the regeneration differences that are largest. Overall the total cycle efficiency varies between ca. 15–30% with the order being $Si > Fe \approx Al > Zn$.

Hazards

In the current study of hazards, we concentrate on the main one associated with transportation and processing, i.e. explosions. Thus this study does not address human factors such as health risks and biological interactions. As specified above, the process also requires capturing metal oxide particles which themselves are also associated with hazards in handling. These are similar to the fly ash generated in coal combustors. However as we shall see, the primary hazard relates to the diameter and explosion risk of the metal particles on which we concentrate here.

Dust explosions

The main issue identified in the transport and handling of powders is the safety risk related to combustible dust. Combustible dust can cause three types of hazards: smouldering fires, flash fires and dust explosions [25]. Dust explosions are treated since these are the most severe hazard.

Unlike flammable gas explosions, which only require fuel, oxygen and ignition, dust explosions require the presence of two additional components: confinement and dispersion. The absence of one of these additional components eliminates the risks of explosion, but a flash fire (deflagration without significant pressure increase) or smouldering slow combustion (associated with low rates of energy release with heat dissipation and thus a non-explosive reaction) can still occur [25].

An explosion can occur either as a:

- deflagration, when the flame front propagates at subsonic velocity and is diffusion limited. A typical flame velocity of a deflagration of metal powder-air mixture is approximately 10–40 cm s^{-1} [1]
- detonation, when the flame front travels at sonic velocities. The dispersed particles ahead of the flame front are auto-ignited by compression due to the shock wave. However these need to be confined: Detonation velocities are typically 10 times or more faster than deflagration velocities.

A dust explosion detonation always originates from a primary dust deflagration [26–29]. The data used in this study is derived from experiments executed in 20 L experimental vessels [30–32] and thus relate to deflagrations. No detailed comparative studies of metal powder detonations are available. This is due to the fact that a detonation cannot develop on the scale under which experiments are carried out. The envisaged bulk shipping scale is much larger, but the chance of a detonation is very low because a very extensive spatial extent of particle dispersion is required and this by definition would not be the case during safe transportation. Moreover, dust particles have to be sufficiently small to detonate [28] – a lot smaller than the particle diameter considered in this study. Given these factors, only deflagrations are considered in this study.

Explosion severity

A characteristic property of an explosion is the sudden increase in pressure. Two essential properties of the pressure trace can be derived from experiments:

- the maximum explosion pressure, MEP or p_{max}: the maximum pressure achieved during an explosion; and
- the maximum rate of pressure rise, MRP or $(dp/dt)_{max}$: the maximum value of the first order derivative of the pressure trace.

Previous workers [33,34] have defined a deflagration index K_{st} given by

$$K_{st} = V^{\frac{1}{3}} \cdot \left(\frac{dp}{dt}\right)_{max} \tag{10}$$

(St stands for “Staub” – German for dust). This enables measurements in a small vessel to be scaled up to larger volumes (assuming that there is no possibility for transition to detonation). The deflagration index K_{st} expresses the intensity of an explosion – note the unit W m^{-2} in Eq. (10) i.e. flux of heating rate from an explosion. K_{st} is classified in three categories of explosions: weak: $K_{st} < 200$; strong: $200 < K_{st} < 300$; and very strong: $K_{st} > 300$.

A relatively simple analysis (see appendix) shows that K_{st} has a dependence on the inverse of the particle diameter i.e. 1/d and this is

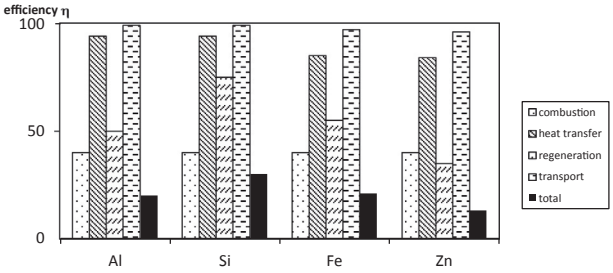

Fig. 5. Efficiencies for different elements in the metal powder cycle for power generation.

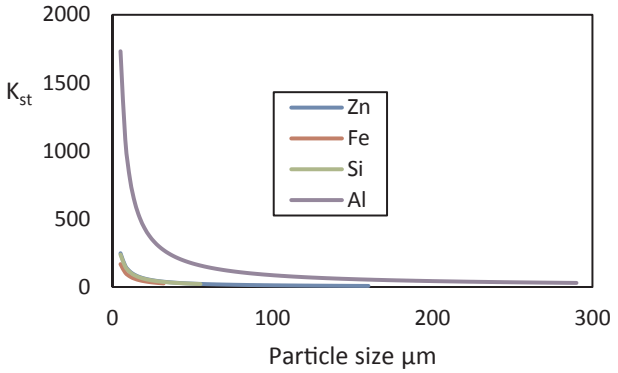

Fig. 6. The deflagration index as a function of particle size. Only Al stands out from the other materials which all overlap – see text [30–34].

used to approximate all the experimental data from other studies [30–34].

The curves for the four materials are summarised in Fig. 6 with a 1/d fit extrapolated fit. The deflagration index K_{st} decreases non-linearly with increasing particle diameter. So, the severity of the explosion can be reduced by increasing the average particle diameter. The Fe, Si and Al lines fall very close to one another and overlap – only Al has a separate curve. It shows values in the strong and very strong explosion range for smaller particle diameters. So for Al the particle diameter should not be less than approximately 50 µm to reduce the severity of an explosion. It is clear that Si, Fe and Zn are not going to be problematic from an explosion hazard point of view. This can be seen by comparing iron (comparable to Zn and Si from the explosibility hazard point of view) and aluminium, along with two traditional energy sources – coal and natural gas.

Eq. (10) shows that there is a dependence on the volume of containment and thus the concentration of particles. Fig. 7 elaborates on the $K_{st} = 200$ safety boundary discussed above. We have averaged all data available which was for particles in ranges below 50 µm. Note that we did not find any data on Si. For Al the range is 5–15 µm and for Fe it is 1–8 µm. Since these are on the rising asymptote from the previous study we can make a comparison. We have also added a comparison with coal dust with average diameter 30 mµ in Fig. 7. In this plot, the deflagration index is plotted as a function of the dust concentration. Because the cubic law (Eq. (10)) also holds for gas explosions, methane is also incorporated in the comparison. Note that the range of this plot is entirely in the weak explosion range ($K_{st} < 200$). From Fig. 7 it is clear that an Al explosion, with particles smaller than approximately 50 µm, is significantly more severe than a methane or coal explosion. Also, the explosion severity is dependent on the concentration, so an Al explosion will only reach the very strong explosion range if both the particle diameter and concentration are in a restricted range.

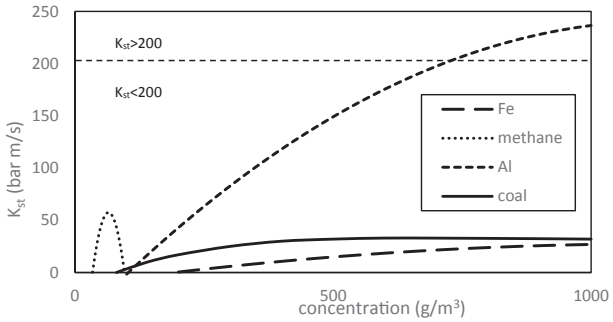

Fig. 7. Deflagration index K_{st} as a function of concentration c (g/m^3) in air [23–25]

Conclusion

1. The shipping requirements for a power plant are comparable to coal for Al and Si powders but more than 4 times higher for iron and zinc.
2. The fact that the metal-oxide powder resulting from combustion is captured increases required shipping capacity by typically 50% for Al and Si but only ca. 30% for Fe and Zn.
3. Overall cycle efficiencies are in the range 15–30%.
4. Handling of metal powders can be done in a safe manner when the particle size is kept above about 25 µm. Care should be taken when handling aluminium as it has the highest deflagration index, which is considerably higher than those of the other metals.
5. Considering availability, transportability, safety and ease of operation preventing aerosols during combustion, we conclude that iron and silicon are preferred candidates for future testing and development of an energy cycle based on metal powders as dense energy carriers.
6. The analysis of the complete cycle has inevitably been subject to much simplification. For example the comparison with coal combustion – in terms of reactants and products – is made at several points. This is useful for an initial evaluation such as this, but there are clear differences which would have to be explored in a more detailed study.

Acknowledgements

This work was funded by Shell Global Solutions International B.V.

A

The MRP depends on the volume of well mixed powder and air. This relationship can be derived from the differential form of the ideal gas law for n moles of gas (mostly nitrogen).

$$nR\frac{\partial T}{\partial t} = p\frac{\partial V}{\partial t} + V\frac{\partial p}{\partial t} \tag{A1}$$

The first term on the right hand side is equal to zero since the dust explodes in a confined space (volume V containing air and particles). Thus with rearrangement we obtain

$$\frac{\partial p}{\partial t} = \frac{nR}{V}\frac{\partial T}{\partial t} = \frac{\rho_g}{M_g}R\frac{\partial T}{\partial t} \tag{A2}$$

where we have used the ideal gas identity $\frac{n}{V} = \frac{\rho_g}{M_g}$ where ρ_g is the gas density and M_g is the molecular weight. The temperature is related to the internal energy (E) by

$$\frac{\partial E}{\partial t} = c_v V\frac{\partial T}{\partial t} \tag{A3}$$

Substituting Eqs. (A3) into (A2) yields

$$\frac{\partial p}{\partial t} = \frac{\rho_g}{M_g}\frac{R}{c_v}\frac{1}{V}\frac{\partial E}{\partial t} \tag{A4}$$

The change in internal energy comes from the heat generated by combustion of the metal particles

$$\frac{\partial E}{\partial t} = \rho_s A_s S_f H V_s \tag{A5}$$

where A_s is the surface area of the particles, S_f the flame speed and ρ_s is the metal density. Inserting Eqs. (A5) into Eq. (A4) gives

$$\frac{\partial p}{\partial t} = \frac{\rho_g}{M_g}\frac{R}{c_v}\rho_s S_f H V_s \frac{A_s}{V} \tag{A6}$$

If there are N particles of diameter d in the volume V, then the total surface area and the volume respectively are given by

$$A_s = NA_p; \quad V = \frac{NV_p}{f} \tag{A7}$$

where f is the volume fraction of metal $f = V_s/V$ in the mixture. For monodisperse spheres this yields

$$\frac{A_S}{V} = \frac{6f}{d} \tag{A8}$$

which inserted into eq. (A6) finally yields

$$\frac{\partial p}{\partial t} = \frac{6f\rho_g}{M_g}\frac{R}{c_v}\rho_s S_f H V_s \frac{1}{d} \tag{A9}$$

References

[1] Bergthorson JM, Goroshin S, Soo MJ, Julien P, Palecka J, Frost DL, et al. Direct combustion of recyclable metal fuels for zero-carbon heat and power. Appl Energy 2015;160:368–82.
[2] Diesel R. Theorie und Konstruktion eines rationellen Wärmemotors zum Ersatz der Dampfmaschine und der heute bekannten Verbrennungsmotoren (1886). Dusseldorf DE: VDI Verlag GmbH; 1991.
[3] Holusha J. GM displays car fueled with coal dust. New York Times; 1981.
[4] Yetter RA, Risha GA, Son SF. Metal particle combustion and nanotechnology. Proc Combust Inst 2009;32(2):1819–38.
[5] Shkolnikov EI, Zhuk AZ, Vlaskin MS. Aluminum as energy carrier: feasibility analysis and current technologies overview. Renewable Sustainable Energy Rev 2011;15(9):4611–23.
[6] Auner N, Holl S. Silicon as energy carrier – facts and perspectives. Energy 2006;31(10):1395–402.
[7] Glassman I, Yetter RA. Combustion. 4th ed. Burlington: Academic Press; 2008. p. 495–550.
[8] Huang X, Gao T, Pan X, Wei D, Lv C, Qin L, et al. A review: feasibility of hydrogen generation from the reaction between aluminum and water for fuel cell applications. J. Power Source 2013;229:133–40.
[9] Bergthorson JM, Yavor Y, Palecka J, Georges W, Soo M, Vickery J, et al. Metal-water combustion for clean propulsion and power generation. Appl Energy 2017;186:13–27.
[10] Bergthorson JM. Recyclable metal fuels for clean and compact zero-carbon power. Prog. Energy Comb. Sci. 2018;68:169–96.
[11] Swamy AKN, Shafirovich E. Conversion of aluminium foil to powders that react and burn with water. Combust Flame 2014;161:322–31.
[12] Mattison T, Lyngfelt A, Cho P. The use of iron oxide as an oxygen carrier in chemical-looping combustion of methane with inherent separation of CO_2. Fuel 2001;80(13):1953–62.
[13] Beckstead MW. A summary of aluminum combustion, NATO Proc. RTO/VKI "Internal aerodynamics in solid rocket propulsion" RTO-EN-023 5:1–46.
[14] Kumar A, Swamy N, Shafirovich E. Conversion of aluminum foil to powders that react and burn with water. Combust Flame 2014;161:322–31.
[15] Li C, Hu C, Xin X, Li Y, Sun H. Experimental study on the operation characteristics of aluminum powder fueled ramjet. Acta Astronaut 2016;129:74–81.
[16] Kramer G-J, Haigh M. No quick switch to low-carbon energy. Nature 2009;462(3):568–9.
[17] Yavor Y, Goroshin S, Berghorson JM, Frost DL. Int J Hydrogen Energy 2015;40:1026–36.
[18] Bouillard J, Vignes A, Dufaud O, Perrin L, Thomas D. Ignition and explosion risks of nanopowders. J Hazard Mater 2010;181(1–3):873–80.
[19] Song C, Wang P, Makse HA. A phase diagram for jammed matter. Nature 2008;453(7195):629–32.
[20] Palumbo R, Diver RB, Larson C, Coker EN, Miller JE, Guertin J, et al. Solar thermal decoupled water electrolysis process 1: proof of concept. Chem Eng Sci 2012;84:372–80.
[21] Hasanbeigi A, Price L, Chunxia Z, Aden N, Xiuping L, Fangqin S. Comparison of iron and steel production energy use and energy intensity in China and the U.S. J Cleaner Prod 2014;65:108–19.
[22] International aluminium institute (IAI), Current IAI statistics 30th June 2016: Primary aluminium smelting intensity. http://www.world-aluminium.org/statistics/primary-aluminium-smelting-energy-intensity/.
[23] Gielen DJ, Van Dril AWN. The basic metal industry and its energy use. Netherlands Energy Research Foundation ECN; 1997. Technical report.
[24] Noteboom T, Cariou P. Fuel surcharge practices of container shipping lines: is it about cost recovery or revenue making? Proceedings of the 2009 International Association of Maritime Economists (IAME) Conference. Denmark: IAME Copenhagen; 2009. p. 24–6.
[25] Ogle RA. Chapter 1 – introduction to combustible dust hazards. In: Ogle Russell A, editor. Dust explosion dynamics. Butterworth-Heinemann34; 2017. p. 1.
[26] Lee JHS, Zhang F, Knystautas R. Propagation mechanisms of combustion waves in dust-air mixtures. Powder Technol 1992;71(2):153–62.
[27] Liu Q, Li X, Bai C. Deflagration to detonation transition in aluminum dust–air mixture under weak ignition condition. Combust Flame 2009;156(4):914–21.
[28] Tulis AJ, Selman JR. Detonation tube studies of aluminum particles dispersed in air. In: Symposium (International) on Combustion, 19(1):655–663, 1982. 19th Symp. (Intl.) Comb.
[29] Sichel M, Kauffman CW, Li YC. Transition from deflagration to detonation in layered dust explosions. Process Safety Progress 1995;14(4):257–65.
[30] Cashdollar KL, Zlochower IA. Explosion temperatures and pressures of metals and other elemental dust clouds. J Loss Prev Process Ind 2007;20(4–6):337–48.
[31] Jacobson M, Cooper AR, Nagy J. Explosibility of metal powders. Bureau of mines: Technical report; 1964.
[32] Cashdollar KL. Coal dust explosibility. J Loss Prev Process Ind 1996;9(1):65–76.
[33] Hertzberg M, Zlochower IA, Cashdollar KL. Metal dust combustion: explosion limits, pressures and temperatures. In: 24th Symp. (Intl.) Combustion 1827-1835; 1992.
[34] Cashdollar KL. Overview of dust explosibility characteristics. J Loss Prev Proc Ind 2000;13:183–99.